THE UNIVERSITY OF
WARWICK

University of Warwick institutional repository: http://go.warwick.ac.uk/wrap

This paper is made available online in accordance with publisher policies. Please scroll down to view the document itself. Please refer to the repository record for this item and our policy information available from the repository home page for further information.

To see the final version of this paper please visit the publisher's website. Access to the published version may require a subscription.

Author(s): T. Kobayashi, C. F. McConville, G. Dorenbos, M. Iwaki, and M. Aono
Article Title: Depth profile and lattice location analysis of Sb atoms in Si/Sb(δ-doped)/Si(001) structures using medium-energy ion scattering spectroscopy
Year of publication: 1999
Link to published version: http://dx.doi.org/10.1063/1.122983
Publisher statement: None

APPLIED PHYSICS LETTERS VOLUME 74, NUMBER 5 1 FEBRUARY 1999

Depth profile and lattice location analysis of Sb atoms in Si/Sb(δ-doped)/Si(001) structures using medium-energy ion scattering spectroscopy

T. Kobayashi[a)]
The Institute of Physical and Chemical Research (RIKEN), Wako, Saitama 351-0198, Japan

C. F. McConville
Department of Physics, University of Warwick, Coventry CV4 7AL, United Kingdom

G. Dorenbos and M. Iwaki
The Institute of Physical and Chemical Research (RIKEN), Wako, Saitama 351-0198, Japan

M. Aono
The Institute of Physical and Chemical Research (RIKEN), Wako, Saitama 351-0198, Japan and Department of Precision Science and Technology, Osaka University, Suita 565-0871, Japan

(Received 31 August 1998; accepted for publication 23 November 1998)

Medium-energy coaxial impact-collision ion scattering spectroscopy has been used to study the depth profile and lattice location of Sb atoms in Si/Sb(δ-doped)/Si(001) structures prepared by solid phase epitaxy. The Sb atoms are observed to diffuse into the Si capping layer at concentrations much higher than the solubility limit in a Si crystal. In addition, the concentration of diffused Sb atoms does not show a monotonic decrease with increasing distance from the δ-layer plane. The lattice locations of the diffused Sb atoms are found to be strongly dependent on the distance from the location of the original Sb δ layer. © *1999 American Institute of Physics.*
[S0003-6951(99)00804-9]

Recently, we have developed medium-energy coaxial impact-collision ion scattering spectroscopy (ME-CAICISS) using a time-of-flight (TOF) energy analyzer, as a method that can be used to analyze the structure and composition of buried interfaces in the near-surface region of materials.[1–5] This is a particularly useful technique for the study of shallow interfaces in semiconductor materials because of their relatively open lattice structure. Using ME-CAICISS, a pulsed ion beam with a medium energy of about 100 keV is incident upon a sample and backscattered particles are detected in a small solid angle around a scattering angle of 180°, corresponding to perfect backscattering, and are energy analyzed using a time-of-flight (TOF) energy analyzer.[1–3]

We have applied ME-CAICISS to observe Sb atoms, initially deposited in a delta (δ)-doped at the interface between a crystalline Si(001) substrate and an amorphous (a)-Si cap, diffuse as a result of postannealing during solid-phase epitaxy (SPE) of the Si capping layer. The purpose of the present work is to investigate the behavior of Sb atoms in a Si/Sb(δ-doped)/Si structure.

In this letter we describe experiments performed on two Sb δ-doped Si samples. The Sb δ-doped Si(001) samples with 25 and 15 nm thick Si capping layers are referred to as samples A and B, respectively. The samples were prepared in the following manner; after the desorption of the surface oxide layer in vacuum, epitaxial Si buffer layers of about 25 nm thickness were formed on clean Si(001) substrates at $\sim 600\,°C$ at a Si deposition rate of about 0.1 nm/s. Then, a small amount of Sb, about 0.6 ML ($1\,ML = 6.78 \times 10^{14}\,atoms/cm^2$), was deposited on the buffer layer also at 600 °C. Next, the Sb δ layer was covered with an a-Si capping layer deposited at room temperature, 25 nm thick for sample A and 15 nm thick for sample B. Finally, the samples were postannealed, for 30 min at 750 °C for sample A and 25 minutes at 650 °C for sample B.

Figure 1(a) shows typical TOF spectra for sample A. The spectra $s2$ shown in Figs. 1(a) and 1(b) were obtained along a random direction. For the purpose of reference, spectra obtained in the [001] aligned direction are also shown as spectra $s1$ in Figs. 1(a) and 1(b). From spectrum $s2$, the concentration of Sb can be calculated as a function of the

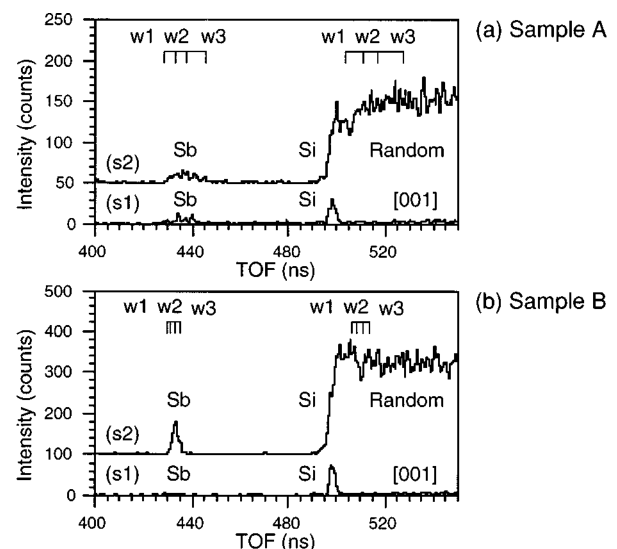

FIG. 1. TOF spectra of (a) sample A and (b) sample B measured in random and [001] aligned directions. TOF windows, w1, w2, and w3 indicated in (a) correspond to sampling depth ranges of 6.5–12, 12–15, and 15–25 nm, respectively, and those in (b) to 9–11, 11–13, and 13–15 nm, respectively.

a)Electronic mail: tkoba@postman.riken.go.jp

 © 1999 American Institute of Physics
Downloaded 06 Jul 2009 to 137.205.202.8. Redistribution subject to AIP license or copyright; see http://apl.aip.org/apl/copyright.jsp

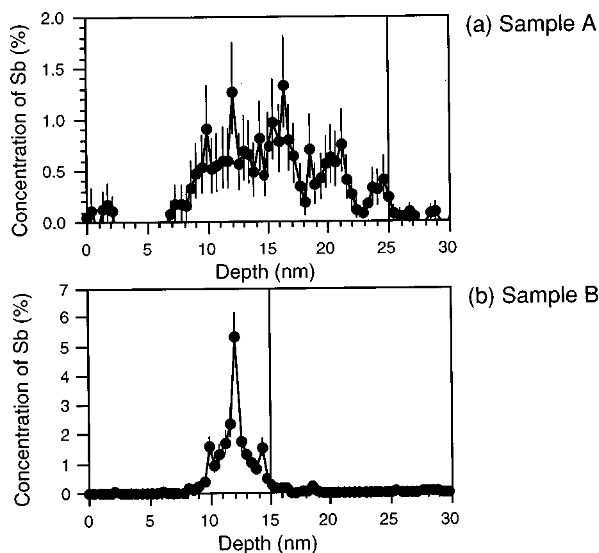

FIG. 2. Depth profiles of the Sb concentration in (a) sample A and (b) sample B. The vertical lines at a depth of 25 nm in (a) and that at 15 nm in (b) indicate the positions of the original Sb δ layer.

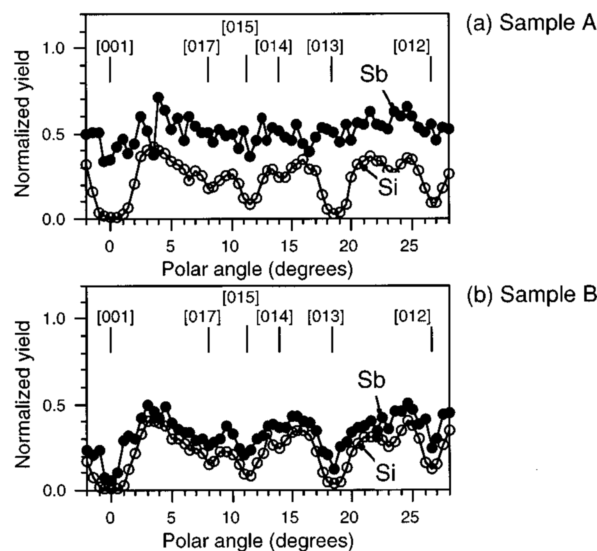

FIG. 3. Intensities of He particles backscattered from Sb atoms (filled circles) and Si atoms (open circles) measured against the polar angle for (a) sample A and (b) sample B. The sampling depth ranges were 6.5–25 nm in (a) and 9–15 nm in (b). In both cases, the polar angle was changed in the (010) azimuthal plane.

depth from the sample surface with the aid of the corresponding stopping power data for He on Si.[6] The result of this calculation is shown in Fig. 2(a), where the vertical line at a depth of 25 nm indicates the position of the original Sb δ layer. As can be seen, Sb atoms have diffused only into the Si cap layer over a distance of about 18 nm.

Figure 1(b) shows a typical TOF spectra for sample B. From the spectrum $s2$ in Fig. 1(b), it is possible to calculate the concentration of Sb as a function of depth, as shown in Fig. 2(b), where again the vertical line, this time at a depth of 15 nm, indicates the position of the original Sb δ layer. In this case, too, Sb atoms have diffused into the Si cap layer, although their distribution is limited to a small thickness of about 6 nm as a result of the lower annealing temperature of sample B (650 °C) as compared to that of sample A (750 °C).

The Sb concentrations observed are much larger than the solubility limit of Sb of approximately 0.05% in a Si crystal at the corresponding annealing temperatures of 650 and 750 °C.[7] In addition, in both Figs. 2(a) and 2(b), the Sb concentration does not show a monotonic decrease with increasing distance from the original Sb δ layer, but rather shows a redistribution of Sb values in a region close to the original δ layer.

In order to analyze the lattice locations of the additional (or supersaturated) Sb atoms in the Si capping layers, the angular dependence of the spectral intensities for the backscattered particles from Sb and Si atoms have been measured. Figure 3(a) shows the backscattered intensities from Sb atoms (filled circles) and Si atoms (open circles) in sample A, measured by changing the polar angle in the (010) azimuthal plane. In all cases the intensities have been normalized with respect to a random direction at every polar angle. These intensity variations for Sb and Si were measured in two TOF windows corresponding to the same sampling depth range of 6.5–25 nm, which cover the entire Sb distribution in sample A as seen in Fig. 2(a). Similar results for sample B are shown in Fig. 3(b). In this case, the intensity variations for Sb and Si were measured in TOF windows corresponding to a sampling depth range of 9–15 nm, which covers the entire Sb distribution in sample B as seen in Fig. 2(b). By comparing Figs. 3(a) and 3(b), it can be seen that the intensity variations in the Si signals are almost identical, with clear intensity drops at the low index or channeling directions. This is typical of a well-crystallized Si(001) sample.

In Fig. 3(b), the intensity variation for the Sb signal as a function of polar angle is also quite similar to that for Si. This indicates that the Sb atoms, which diffused into the Si cap layer of sample B, are mostly situated at substitutional sites in the Si lattice. In contrast to this, Fig. 3(a) shows almost no intensity variation in the Sb signal and shows little correlation with the Si signal. The Sb signal is almost constant and at a higher intensity level. This indicates that a large fraction of Sb atoms that have diffused into the Si capping layer of sample A are not situated at substitutional sites.

This observation can be interpreted on the basis of Figs. 4(a) and 4(b). Figure 4(a) shows the intensity variations for Sb (top panel) and Si (bottom panel) in a manner similar to Fig. 3(a). The plots are produced for three subdivided depth ranges of 6.5–12 nm (circular symbols), 12–15 nm (square symbols), and 15–25 nm (triangular symbols) for sample A. Figure 4(b) also shows similar plots for three subdivided depth ranges for sample B, this time of 9–11 nm (circular symbols), 11–13 nm (square symbols), and 13–15 nm (triangular symbols). In both Figs. 4(a) and 4(b), the intensity variations for Si in the three different depth ranges are quite similar, indicating that the Si cap layers of samples A and B are well crystallized at all depths. Strictly speaking, a more careful observation of the data reveals that the crystalline quality (i.e., the degree of atomic order) of the Si capping layer is slightly poorer for sample B and can be attributed to the lower annealing temperature (650 °C). It is also observed that the crystalline quality of the Si cap layers is slightly better in the deeper regions of the samples, espe-

Downloaded 06 Jul 2009 to 137.205.202.8. Redistribution subject to AIP license or copyright; see http://apl.aip.org/apl/copyright.jsp

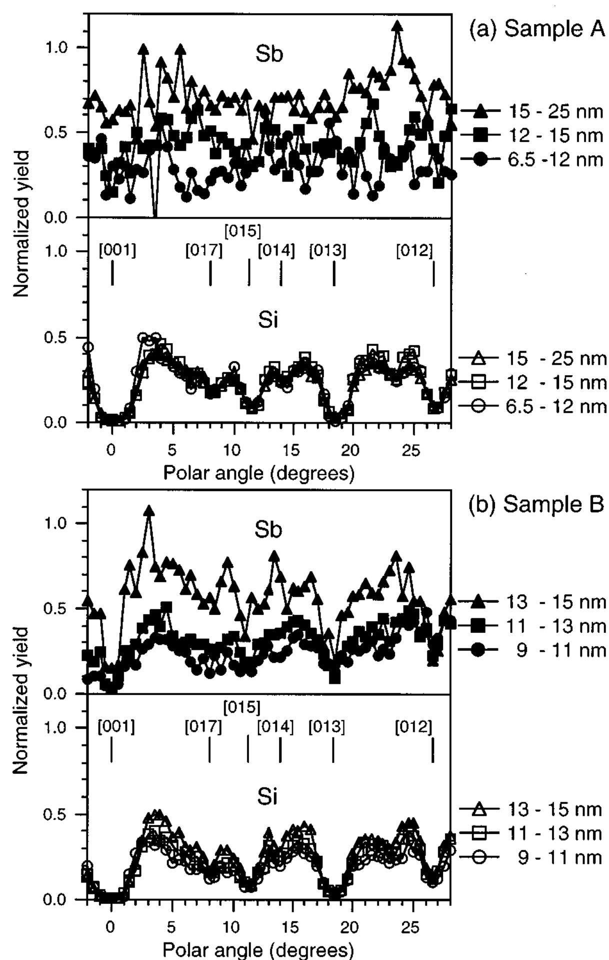

FIG. 4. Angular dependency of the backscattered He particles from Sb and Si atoms in (a) sample A and (b) sample B similar to Figs. 3(a) and 3(b). The plots are produced for three subdivided sampling depth ranges: 6.5–12 nm (circular symbols), 12–15 nm (square symbols), and 15–25 nm (triangular symbols) in (a); and 9–11 nm (circular symbols), 11–13 nm (square symbols), and 13–15 nm (triangular symbols) in (b).

cially in sample B. This suggests that the crystallization of the Si cap layers began either at a greater depth in the sample or at the position of the Sb δ layers in the Si substrate and then progressed toward the surface.

In Fig. 4(b), the intensity variations for Sb in shallow regions with depths of 9–11 and 11–13 nm are shown for sample B and are quite similar to those of Si. However, the intensity variation at depths of 13–15 nm is very different from those of Si. This implies that Sb atoms in the shallow regions are mostly situated at substitutional sites on the Si lattice, but only a small part of Sb atoms occupy substitutional sites in the deeper region. A similar tendency is also observed in Fig. 4(a) for sample A, although the fraction of Sb atoms at substitutional sites is smaller in this case than in the case of sample B, since the observed intensities are larger in sample A than in sample B. Remembering that the local crystalline quality of the Si cap layers is better in deeper regions in both samples A and B, and that the averaged crystalline quality is better in sample A than in sample B, these results would suggest that the Sb atoms in the Si cap layers tend to occupy more substitutional sites in a region with a lower degree of crystalline quality. That is to say, the Sb atoms would tend to be ''pushed out'' of substitutional sites in a region where the overall crystalline quality is somewhat better. This is consistent with reported experimental results on the implantation of Sb atoms into a Si crystal.[8,9]

It is proposed that SPE of the Si cap layer and the diffusion of the δ-doped Sb atoms during the postannealing proceeds in the following steps. Initially, the Sb atoms in the δ layer rapidly diffuse into the Si capping layer. Since the Si cap layer is not well crystallized, the Sb atoms can diffuse, easily passing through random interatomic positions. The concentration of Sb atoms diffusing into the a-Si cap layer can, therefore, be larger than the solubility limit of Sb in a Si crystal. At this point, the concentration of Sb atoms will show a monotonic decrease with increasing distance from the original Sb δ-layer plane. During the initial stage of postannealing, the Si cap layer is gradually crystallized. The crystallization begins at the original position of the Sb δ layer, where nucleation for crystallization is promoted by the presence of the Si(001) crystalline substrate, and then progresses toward the surface. When a region close to the original position of the Sb δ layer is first crystallized, the solubility limit of Sb in the region decreases and some of the Sb atoms in this region are driven to a neighboring region where the degree of crystallization is lower and, therefore, the solubility limit of Sb is larger. This process continues as postannealing proceeds. When the Si capping layer is crystallized, Sb atoms in the layer are first incorporated at the substitutional sites of the Si lattice, since the Si lattice can accommodate the Sb atoms at substitutional sites when the lattice has a high concentration of residual defects. As postannealing proceeds further, the crystalline quality of the Si cap layer improves and a larger fraction of the Sb atoms are removed from substitutional sites. Since the crystalline quality is better in regions closer to the original Sb δ layer, where crystallization begins earlier, the fraction of Sb atoms at substitutional sites is smaller in these regions.

To summarize, ME-CAICISS has been successfully applied to understand microscopic mechanism of diffusion of Sb atoms δ-doped between an Si(001) substrate and an a-Si capping layer during SPE of the capping layer.

[1] T. Kobayashi, S. Shimoda, M. Iwaki, and M. Aono, RIKEN Rev. **12**, 33 (1996).

[2] T. Kobayashi, T. Utiyama, K. Takagi, M. Iwaki, and M. Aono, Abstracts of the 12th International Vacuum Congress (IVC-12) and the 8th International Conference on Solid Surfaces (ICSS-8), The Hague, Oct., 1992, SS-ThP31.

[3] T. Kobayashi, T. Utiyama, K. Takagi, M. Iwaki, and M. Aono, Abstracts of the 53rd Autumn Meeting of the Jpn. Soc. Appl. Phys., Suita, Sept., 1992, 18pZW10.

[4] T. Kobayashi, G. Dorenbos, M. Iwaki, and M. Aono (unpublished).

[5] T. Kobayashi, G. Dorenbos, S. Shimoda, M. Iwaki, and M. Aono, Nucl. Instrum. Methods Phys. Res. B **118**, 584 (1996).

[6] J. F. Zieglar, *Helium Stopping Powers and Ranges in All Element Matter, Stopping and Ranges of Ions in Matter* (Pergamon, New York, 1977), Vol. 4.

[7] F. A. Trumbore, Bell Syst. Tech. J. **39**, 205 (1960).

[8] O. J. Marsh, J. W. Mayer, G. A. Shifrin, and D. Jamba, Appl. Phys. Lett. **11**, 92 (1967).

[9] J. A. Davies, J. Denhartog, L. Eriksson, and J. W. Mayer, Can. J. Phys. **45**, 4053 (1967).

Downloaded 06 Jul 2009 to 137.205.202.8. Redistribution subject to AIP license or copyright; see http://apl.aip.org/apl/copyright.jsp